Using Proton Irradiation to Probe the Origins of Low-Frequency Noise Variations in SiGe HBTs

Zhenrong Jin, Jarle A. Johansen, John D. Cressler, Robert A. Reed, Paul W. Marshall, and Alvin J. Joseph

Abstract—We use proton irradiation to probe the origins of the geometry-dependent variation of low-frequency noise in 120 GHz SiGe heterojunction bipolar transistors (HBTs). Before irradiation, small-sized transistors show a strong variation in noise magnitude across many samples, whereas the noise in larger devices is more statistically reproducible. Although the noise magnitude shows little degradation after 2×10^{13} p/cm^2 irradiation, the observed noise variation decreases. Its dependence on both geometry and bias is quantified. This fundamental geometrical scaling effect is investigated using theoretical calculations based on the superposition of generation/recombination (G/R) noise sources.

Index Terms—Bipolar transistors, heterojunction bipolar transistor (HBT), low-frequency noise, $1/f$ noise, proton irradiation, SiGe.

I. INTRODUCTION

SiGe heterojunction bipolar transistor (HBT) bipolar complementary metal–oxide–semiconductor (BiCMOS) technology offers high-level integration, low cost, and high-speed, and is being increasingly used for mixed-signal circuit applications. Low-frequency noise (LFN) in transistors usually has a $1/f$-like spectrum, and sets the lower limit on the detectable signal level, not only in the low frequency range, but also at high frequencies via the up-conversion to the carrier frequency through the nonlinearities of the device (phase noise). Understanding LFN is thus a crucial design issue in direct-conversion receivers, oscillators, synthesizers, amplifiers, and mixers for digital, analog and optoelectronics applications.

Transistors are aggressively scaled (down-sized) in order to improve performance and integration level. One design issue associated with geometrical scaling is that the LFN often shows a different frequency dependence for each individual device [1], [2], and this can directly affect both circuit performance and accurate compact modeling. This LFN variation has been observed in BJTs and SiGe HBTs in very small-sized devices
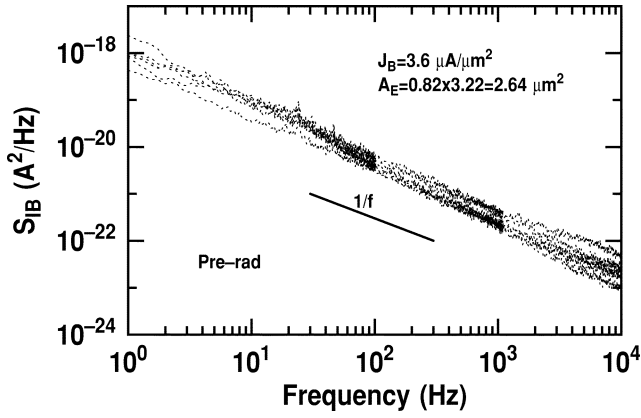
[1], [2], and the fundamental mechanism is regarded to be the superposition of individual trapping/detrapping processes due to the presence of G/R centers in the device. Each G/R center contributes a Lorentzian-type $(1/f^2)$ noise signature. Given a sufficient number of traps and a particular distribution of characteristic time constants associated with the G/R centers, these Lorentzian processes combine to produce the observed $1/f$ noise behavior [3]. At sufficiently small size, however, the total number of traps is small enough that non-$1/f$ behavior, and large statistical variations, can be observed. These trapping/detrapping processes modulate the number of carriers and, thus, are best described by number fluctuation theory [1]–[13] instead of mobility fluctuation theory [14]–[18].

In this work, we intentionally introduce additional traps into the transistor via proton irradiation in order to probe the physical origins of the observed LFN variations in 120 GHz SiGe HBTs. In addition, this work provides valuable information on whether such LFN variations are potentially important in space-borne communications applications.
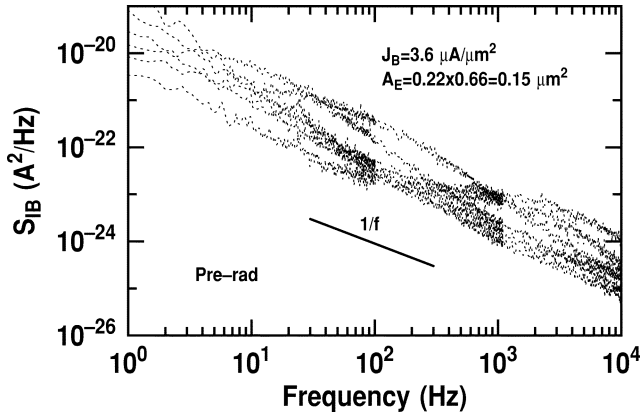
II. EXPERIMENT

The transistors are from a fully integrated, commercially available 0.20 μm 120 GHz peak f_T SiGe technology from IBM [19]. Since the dominant noise source in the common-emitter configuration is associated with the base current, the base current noise spectrum (S_{I_B}) was investigated [1], [2], [6], [7]. The transistor was biased in a common-emitter configuration with $V_{CB} = 0$ V. The details of the noise measurement system can be found in [20]. Transistors with emitter areas (A_E) of 0.82×3.22 μm^2, 0.30×1.86 μm^2 and 0.22×0.66 μm^2 were measured, and are hereafter referred to as "large," "medium," and "small" devices. For meaningful statistical comparisons, six transistors of each transistor size were characterized on separate die from the same wafer.

The samples were diced and attached to a ceramic holder and directly exposed with terminals floating to 62.5 MeV protons at the Crocker Nuclear Laboratory cyclotron located at the University of California at Davis. A total accumulated fluence of 2×10^{13} protons/cm^2 was used. Dosimetry measurements used a 5-foil secondary emission monitor calibrated against a Faraday cup. Ta scattering foils located several meters upstream of the target establish a beam spatial uniformity of 15% over a 2 cm radius circular area. Beam currents from about 5 pA to 50 nA allow testing with proton fluxes from 10^6 to 10^{11} protons/cm^2/s. The dosimetry system has been previously described in [21], [22], and is accurate to about 10%.

Z. Jin and J. D. Cressler are with School of Electrical and Computer Engineering, Georgia Institute of Technology, Atlanta, GA 30332-0250 USA (e-mail: zhenrong@ece.gatech.edu).

J. A. Johansen is with Institute of Physics, University of Tromsø, 9037 Tromsø, Norway.

R. A. Reed is with NASA-GSFC, Greenbelt, MD 20771 USA.

P. W. Marshall is a consultant to NASA GSFC, Greenbelt, MD 20771 USA.

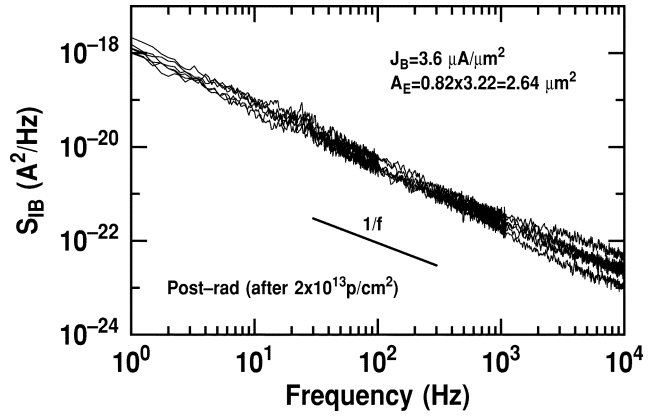A. J. Joseph is with IBM Microelectronics, Essex Junction, VT 05452 USA.

Fig. 1.   (a) Pre-rad noise spectra from large transistors at $J_B = 3.6\,\mu\mathrm{A}/\mu\mathrm{m}^2$. Six samples are shown. (b) Pre-rad noise spectra from small transistors at $J_B = 3.6\,\mu\mathrm{A}/\mu\mathrm{m}^2$. Six samples are shown.

Fig. 2.   (a) Post-rad noise spectra from large transistors at $J_B = 3.6\,\mu\mathrm{A}/\mu\mathrm{m}^2$. Six samples are shown. (b) Post-rad noise spectra from small transistors at $J_B = 3.6\,\mu\mathrm{A}/\mu\mathrm{m}^2$. Six samples are shown.
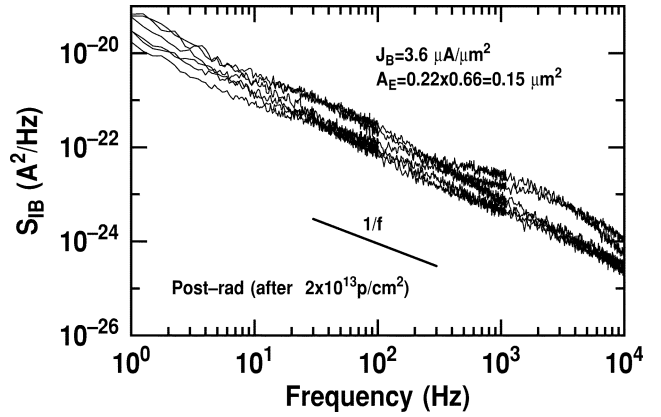
III. MEASUREMENT RESULTS

In Fig. 1, we compare the measured noise spectra from six samples of small and large SiGe HBTs. The devices were biased at the same base current density (J_B) to obtain a similar forward voltage bias on the base-emitter junction. Observe that the noise spectra, shown in Fig. 1, exhibit $1/f^\alpha$ frequency dependences with α close to but slightly larger than unity. This deviation from $1/f$ frequency dependence could be a result of thermally activated processes, as suggested by Dutta–Horn model [23]. Interestingly, we observe a large statistical variation of the LFN spectra between different samples of the small transistors, whereas the large devices show a very similar LFN signature among different samples, consistent with our earlier results on a 90 GHz SiGe technology [2]. Post-radiation noise spectra of small and large SiGe HBTs are compared in Fig. 2. It is clearly seen that noise variation decreases for small devices, but remains nearly the same for large devices. The variation in noise at a spot frequency (a measured single frequency) between the samples of the same geometry was quantified using a variation coefficient (δ), given by the standard deviation formula [1], [2]:

$$\delta = \frac{1}{S_{I_B,\mathrm{avg}}} \sqrt{\frac{1}{N-1} \sum_{i=1}^{N} \left(S_{I_B,i} - S_{I_B,\mathrm{avg}} \right)^2}$$

$$S_{I_B,\mathrm{avg}} = \frac{1}{N} \sum_{i=1}^{N} S_{I_B,i} \tag{1}$$

where i indicates the ith sample, and N is the total number of samples (δ is then averaged over the measurement frequencies).

The observed noise variation before proton irradiation is not strongly dependent on base current density, as can be seen in Fig. 3. This is consistent with our observation of the measured noise spectra, which only increase in magnitude, and not in shape, with increasing bias current. After proton irradiation, however, the noise variation shows a significant decrease for the small devices, especially at low J_B, but shows a smaller decrease for the medium and large devices, as shown in Fig. 3. The noise variation thus now depends both on geometry and bias. It is clear that radiation exposure changes the noise variation in these SiGe HBTs. Interestingly, after irradiation, the average noise magnitude shows little degradation at the three bias current densities for the three geometries, as shown in Fig. 4. Furthermore, if we track the noise spectra of the pre- versus post-irradiated individual devices for the small transistors at low bias current, two of them show an observable noise magnitude change, while the others only show changes in noise spectral shape. This suggests that the changes in the pre- and post-radiation noise spectra is a random process, and should be captured by a statistical model.
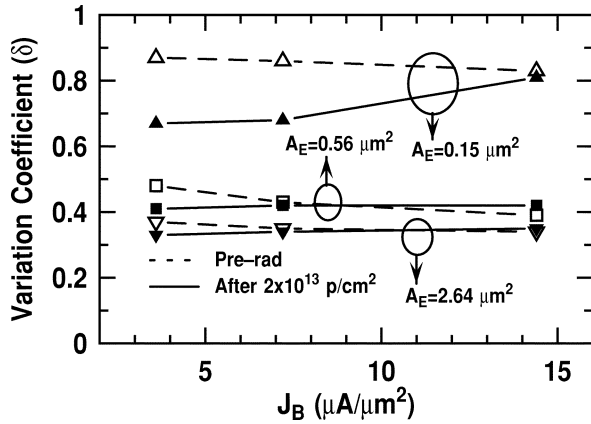
Fig. 3. Noise variation for measured noise spectra versus J_B before and after irradiation. δ is an average value over measurement frequencies.
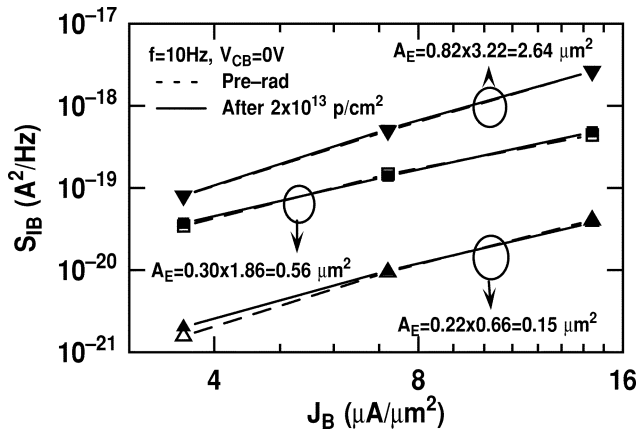

Fig. 5. Noise and dc parameter variations from measured data versus A_E before and after irradiation.

Fig. 4. Noise magnitude versus J_B at 10 Hz before and after irradiation.
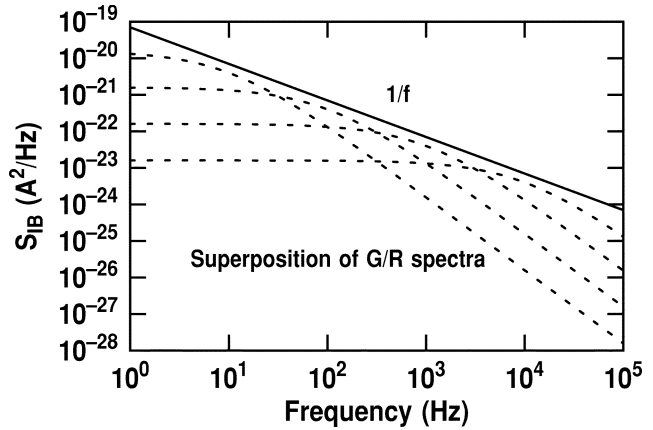
Fig. 6. Superposition of Lorentzian (G/R) spectra yields a $1/f$ spectrum.

The noise was measured with the base current held constant from sample-to-sample. Due to small variations in the dc parameters, we observed slight variations in the base-emitter voltage needed to obtain the desired base current, and also a variation in the resulting collector current due to variations in the current gain at a fixed base current from sample to sample across the wafer. The observed variation in current gain and V_{BE} was also calculated using the standard deviation formula. The results are shown in Fig. 5. The variation in the *dc* parameters is negligible compared to the large variation in the noise, and hence the observed noise variation is clearly not caused by variations in the transistor dc parameters alone.

IV. MODEL AND DISCUSSION

A. Pre-Radiation

An intuitive explanation for the physical basis of carrier number fluctuations in bipolar junction transistors (BJTs) depends on the trapping/detrapping of carriers by traps at the interfaces or oxide layers in the device [9]. The noise of each individual trapping/detrapping process theoretically exhibits a Lorentzian spectrum $(1/f^2)$, which can be expressed as

$$S_{I_B} = \alpha \frac{\tau}{1 + (2\pi f \tau)^2} \quad (2)$$
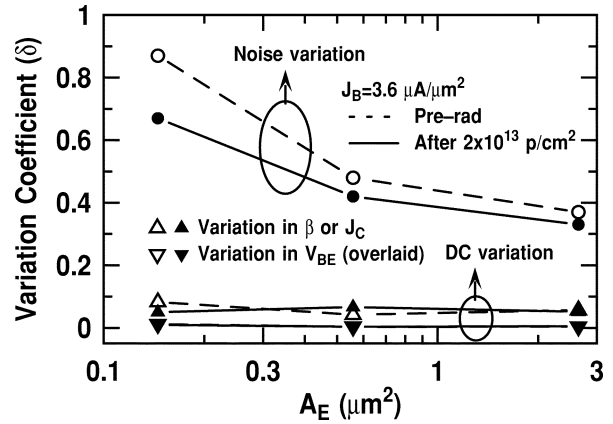
where α is the amplitude (with units of A^2) and τ is the characteristic time constant. The noise spectrum is flat at low frequency and decreases as $1/f^2$ at high frequency. The superposition of a large number of Lorentzian spectra with a $1/\tau$ distribution results in the usually observed $1/f$ spectrum [3], as illustrated in Fig. 6.

In [2], the $1/f$ noise in SiGe HBTs was expressed as the superposition of such Lorentzian noise sources. The pre-rad S_{I_B} depends on bias and geometry, as seen in Fig. 4. The best fit to the data shows a $J_B^{2.4} A_E^{1.2}$ dependence. Following the same procedure outlined in [2], to obtain a best fit to the pre-radiation measurement data, an empirical expression of the low-frequency noise spectrum can be written as [1], [2]

$$S_{I_B} = \sum_i^{N_T} A \frac{A_E^{0.2} J_B^{2.4} \tau_i}{1 + (2\pi f \tau_i)^2} \quad (3)$$

where A is a constant, τ_i is the characteristic time constant of the ith independent traps and has to be distributed as $1/\tau$ to produce a $1/f$ spectrum, and N_T is the total number of characteristic time constants associated with traps in the device and proportional to A_E. When N_T is large enough, which is the case in the large device, (3) yields a $1/f$ spectrum. When N_T is small enough, corresponding to the small device case, the spectrum modeled by this equation will show a deviation from $1/f$ behavior. Five hundred different characteristic time constants
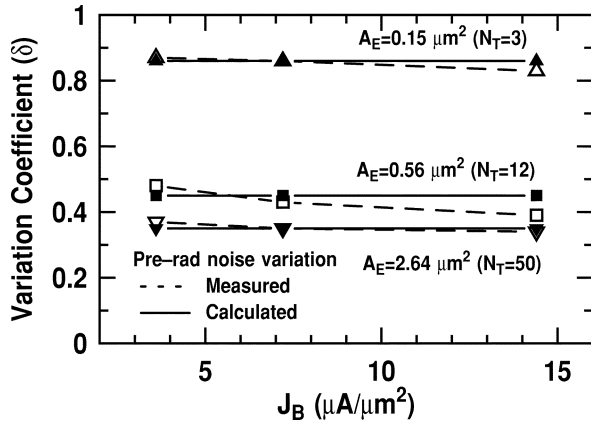
Fig. 7. Noise variation from measured and calculated noise spectra versus J_B before irradiation. The number of traps used in the calculations is indicated for each size.

Fig. 8. I_C and I_B versus V_{BE} for a small transistor before and after irradiation.

were generated over the range $1/(2\pi \times 10^7)$ to $1/(2\pi \times 10^{-3})$ with a $1/\tau$ distribution. To best fit the data, three characteristic time constants were chosen for the small-sized device, 12 were chosen in the medium-sized device, and 50 were chosen in the large-sized device. In the calculation, characteristic time constants were randomly drawn from the previously generated 500 cases, which have a $1/\tau$ distribution, for every calculation of the small, medium, and large devices ($A = 1.1 \times 10^{-23}$).

Six individual calculations (to mimic the six independent measurements) were performed for each size device, and the resultant noise variation coefficient of the six calculated spectra is shown in Fig. 7, which is consistent with the measured data. The calculated noise variation is bias independent as expected from (1) and (3). These calculations indicate that a small number of traps indeed leads to the observed large noise variation in the small devices.

B. Post-Radiation

Proton irradiation generates traps at the Si–SiO$_2$ interface [24] at the E-B spacer around device emitter perimeter [20]. These traps create a nonideal base current component due to increased space-charge region (SCR) G/R center recombination current near the surface, as confirmed in Fig. 8. The dc degradation of SiGe HBTs after proton irradiation has been extensively investigated in [25].

Assuming that the observed radiation-induced noise increase is mainly due to these peripheral traps, the radiation-induced LFN increase $S_{I_B,\mathrm{SCR}}$ can be expressed as [20]

$$S_{I_B,\mathrm{SCR}} = C J_B n_{T,R} P_E \frac{\alpha_H}{f} \tag{4}$$

where C is a constant that is independent of bias and geometry, $n_{T,R}$ is the peripheral trap density induced by radiation, P_E is the emitter perimeter, and α_H is the Hooge constant. Thus, radiation-induced $S_{I_B,\mathrm{SCR}}$ shows an J_B and P_E dependence. By analogy to the pre-radiation behavior, assuming each radiation-induced trap has a Lorentzian spectrum, the radiation-induced noise power spectral density $S_{I_B,\mathrm{SCR}}$ can also be expressed as a superposition of Lorentzian spectra provided that the superposition shows a J_B and P_E dependence when the
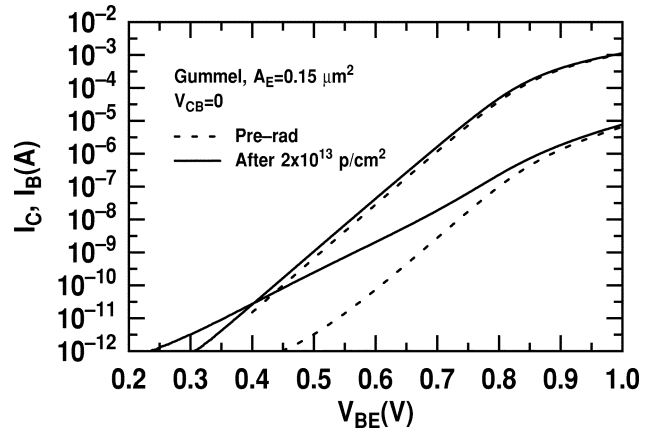
number of traps is large enough, as expected from (4). Hence, an empirical expression for $S_{I_B,\mathrm{SCR}}$ can be obtained as

$$S_{I_B,\mathrm{SCR}} = \sum_{j=1}^{N_{T,R}} B \frac{J_B \tau_j}{1 + (2\pi f \tau_j)^2} \tag{5}$$

where τ_j is the characteristic time constant associated with the jth radiation-induced traps, B is a constant, and $N_{T,R}$ is the number of characteristic time constants associated with traps induced by radiation, which is assumed to be proportional to the emitter perimeter. The post-radiation spectrum can be obtained by adding (3) and (5)

$$S_{I_B,\mathrm{post}} = S_{I_B} + S_{I_B,\mathrm{SCR}} \tag{6}$$

$$= \sum_{i=1}^{N_T} A \frac{J_B^{2.4} A_E^{0.2} \tau_i}{1 + (2\pi f \tau_i)^2} + \sum_{j=1}^{N_{T,R}} B \frac{J_B \tau_j}{1 + (2\pi f \tau_j)^2}. \tag{7}$$

Since S_{I_B} increases much faster than $S_{I_B,\mathrm{SCR}}$ when J_B increases, S_{I_B} can be the dominant term at high bias in (7). It is thus possible to see that the noise variation shows a decrease at low J_B, rather than at high J_B for the same size devices, as shown in Fig. 3. For small devices with a small number of pre-radiation traps and a large noise variation, a few more radiation-induced traps can effectively decrease the noise variation at certain J_B. It is thus possible to see a relatively large decrease of noise variation for small devices compared to the medium and large devices.

To best fit the data, one characteristic time constant associated with radiation-induced traps was added to the small-sized device after irradiation, two were added to the medium-sized one, and five were added to the large-sized one ($B = 5.2 \times 10^{-18}$), consistent with a uniform trap generation rate at the device perimeter. The post-radiation calculation results are shown in Fig. 9, and are in agreement with the measured data. The calculated results of average post-radiation noise magnitude are also close to the data, but for brevity are not shown.

V. SUMMARY

We have investigated for the first time the effects of proton irradiation on the low-frequency noise variation in aggressively-scaled SiGe HBTs. The pre-radiation LFN variation is geometry dependent and largest for the smallest devices, but shows little
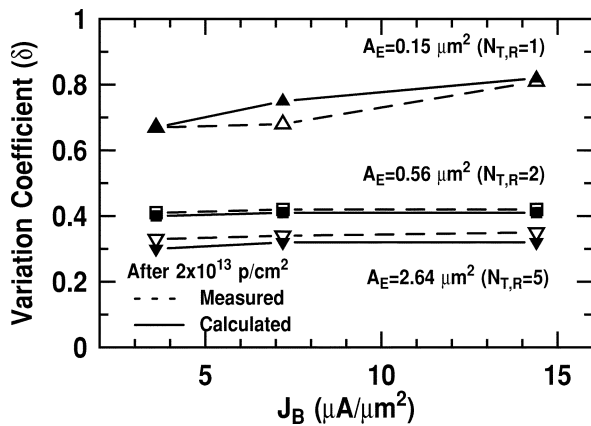
Fig. 9. Noise variation from measured and calculated noise spectra versus J_B after irradiation. The number of additional characteristic time constants associated with radiation-induced traps used in calculations is indicated for each size.

dependence on bias. After irradiation, however, the overall noise magnitude shows little degradation, but the noise variation decreases significantly for the small devices, and shows both geometry and bias dependence.

The pre-radiation noise can be expressed as a superposition of individual G/R traps, and the number of characteristic time constants associated with G/R trap centers is proportional to the area of the transistors. The calculation shows a small number of pre-radiation traps leads to a large noise variation. The radiation-induced noise is written as another set of superposed G/R traps and added to the pre-radiation expression, and the number of characteristic time constants associated with radiation-induced G/R traps is proportional to the emitter perimeter. Calculations show that such radiation-induced traps can decrease the noise variation, consistent with the data.

Advanced device technologies with aggressively-scaled emitter geometries have a size-dependent low-frequency noise variation, and this variation is sensitive to proton irradiation. Proton irradiation can decrease the noise variation without any significant degradation in noise magnitude, and thus favors the application of scaled SiGe HBT technology in the radiation environment. This size variation is believed to be fundamental to scaled bipolar technologies and, thus, is of potential concern for noise-sensitive circuits operating in the radiation environment.

ACKNOWLEDGMENT

REFERENCES

[1] M. Sanden, O. Marinov, and M. J. Deen *et al.*, "A new model for the low-frequency noise and the noise level variation in polysilicon emitter BJTs," *IEEE Trans. Electron Devices*, vol. 49, pp. 514–520, June 2002.

[2] Z. Jin, J. D. Cressler, G. Niu, and A. J. Joseph, "Low-frequency noise variation in scaled SiGe HBTs," in *Proc.'02 Bipolar/BiCMOS Circuits and Technology Meet.* , Monterey, CA, 2002, pp. 224–227.

[3] A. L. McWhorter, "1/f Noise and Related Surface Effects in Germanium,", Boston, MA, Lincoln Laboratory Rep. no. 80, May 1955.

[4] M. J. Uren, D. J. Day, and M. J. Kirton, "1/f and random telegraph noise in silicon MOSFETs," *Appl. Phys. Lett.*, vol. 47, no. 11, pp. 1195–1197, Dec. 1985.

[5] K. Kandiah, "Random telegraph signal currents and low-frequency noise in JFETs," *IEEE Trans. Electron Devices*, vol. 41, pp. 2006–2015, Nov. 1994.

[6] L. S. Vempati, J. D. Cressler, J. A. Babcock, R. C. Jaeger, and D. L. Harame, "Low-frequency noise in UHV/CVD epitaxial Si and SiGe bipolar transistors," *IEEE J. Solid-State Circuits*, vol. 31, pp. 1458–1467, Oct. 1996.

[7] P. Llinares, D. Celi, and O. Roux-dit-Buisson *et al.*, "Dimension scaling of 1/f noise in the base current of quasiself-aligned polysilicon emitter bipolar junction transistors," *J. Appl. Phys.*, vol. 82, no. 5, pp. 2671–2675, 1997.

[8] W. S. Lau, E. F. Chor, C. S. Foo, and W. C. Khoong, "Strong low-frequency noise in polysilicon emitter bipolar transistors with interfacial oxide due to fluctuations in tunneling probabilities," *Jpn. J. Appl. Phys.—Part 2 Lett.*, vol. 31, no. 8A, pp. L1021–L1023, 1992.

[9] M. J. Deen, S. Rumysantesev, R. Bashir, and R. Taylor, "Measurements and comparison of low frequency noise in npn and pnp polysilicon emitter bipolar transistors," *J. Appl. Phys.*, vol. 84, no. 1, pp. 625–633, 1998.

[10] X. Y. Chen, M. J. Deen, Z. X. Yan, and M. Schroter, "Effects of emitter dimensions on low-frequency noise in double-polysilicon BJTs," *Electron. Lett.*, vol. 34, no. 2, pp. 219–220, 1998.

[11] R. Plana, L. Escotte, J. P. Roux, J. Graffeuil, A. Gruhle, and H. Kibbel, "1/f noise in self-aligned Si/SiGe heterojunction bipolar transistor," *IEEE Electron Device Lett.*, vol. 16, pp. 58–60, Feb. 1995.

[12] H. A. W. Markus and T. G. M. Kleinpenning, "Low-frequency noise in polysilicon emitter bipolar transistors," *IEEE Trans. Electron Devices*, vol. 42, pp. 720–727, Apr. 1995.

[13] A. Mounib, F. Balestra, N. Mathieu, J. Brini, G. Ghibaudo, A. Chovet, A. Chantre, and A. Nouailhat, "Low-frequency noise sources in polysilicon emitter BJTs: influence of hot-electron-induced degradation and post-stress recovery," *IEEE Trans. Electron Devices*, vol. 42, pp. 1647–1652, Sept. 1995.

[14] F. N. Hooge, "1/f noise sources," *IEEE Trans. Electron Devices*, vol. 41, pp. 1926–1935, Nov. 1994.

[15] J. Kilmer, A. van der Ziel, and G. Bosman, "Presence of mobility-fluctuation 1/f noise identified in silicon p^+np transistors," *Solid State Electron.*, vol. 26, no. 1, pp. 71–74, 1983.

[16] L. K. J. Vandamme, X. Li, and D. Rigaud, "1/f noise in MOS devices, mobility or number fluctuation," *IEEE Trans. Electron Devices*, vol. 41, pp. 1936–1945, Nov. 1994.

[17] T. G. M. Kleinpenning, "1/f noise in p-n diodes," *Physica B/C*, vol. 98, no. 4, pp. 289–299, 1980.

[18] L. K. J. Vandamme, E. P. Vandamme, and J. J. Dobbelsteen, "Impact of silicon substrate, iron contamination and perimeter on saturation current and noise in n^+p diodes," *Solid State Electron.*, vol. 41, no. 6, pp. 901–908, 1997.

[19] A. J. Joseph, D. Coolbaugh, M. Zierak, R. Wuthrich, P. Geiss, Z. He, X. Liu, B. Orner, J. Johnson, G. Freeman, D. Ahlgren, B. Jagannathan, L. Lanzerotti, V. Ramachandran, J. Malinowski, H. Chen, J. Chu, P. Gray, R. Johnson, J. Dunn, S. Subbanna, K. Schonenberg, D. Harame, R. Groves, K. Watson, D. Jadus, M. Meghelli, and A. Rylyakov, "A 0.18 μm BiCMOS technology featuring 120/100 GHz (f_T/f_{max}) HBT and ASIC-compatible CMOS using copper interconnect," in *Proc.'01 Bipolar/BiCMOS Circuits and Technology Meet.*, Minneapolis, MN, 2001, pp. 143–146.

[20] Z. Jin, G. Niu, J. D. Cressler, C. J. Marshall, P. W. Marshall, H. S. Kim, R. Reed, and D. L. Harame, "1/f noise in proton irradiated SiGe HBTs," *IEEE Trans. Nucl. Sci.*, vol. 48, pp. 2244–2249, Dec. 2001.

[21] K. M. Murray, W. J. Stapor, and C. Castenada, "Proton beam facility for single event research," *Nucl. Instrum. Methods*, vol. B56/57, p. 616, 1991.

[22] P. W. Marshall, C. J. Dale, M. A. Carts, and K. A. LaBel, "Particle-induced bit errors in high performance fiber optic data links for satellite data management," *IEEE Trans. Nucl. Sci.*, vol. 41, pp. 1958–1965, Dec. 1994.

[23] P. Dutta and P. M. Horn, "Low-frequency fluctuations in solids: 1/f noise," *Rev. Modern Phys.*, vol. 53, pp. 497–516, 1981.

[24] S. N. Rashkeev, D. M. Fleetwood, R. D. Schrimpf, and S. T. Pantelides, "Proton-induced defect generation at the $Si - SiO_2$ interface," *IEEE Trans. Nucl. Sci.*, vol. 48, pp. 2086–2092, Dec. 2001.

[25] J. D. Cressler, R. Krithivasan, G. Zhang, G. Niu, P. W. Marshall, H. S. Kim, R. A. Reed, M. J. Palmer, and A. J. Joseph, "An investigation of the origins of the variable proton tolerance in multiple SiGe HBT BiCMOS technology generations," *IEEE Trans. Nucl. Sci.*, vol. 49, pp. 3203–3207, Dec. 2002.